

A numerical study on baseline-free damage detection using frequency steerable acoustic transducers

Octavio A. Márquez Reyes^{1*} [0000-0002-9853-0629], Beata Zima^{1, 2} [0000-0001-8228-5959],
Jochen Moll¹ [0000-0003-2299-2250], Masoud Mohammadgholiha³ [0000-0003-1597-6295],
Luca de Marchi³ [0000-0003-0637-9472]

¹ Department of Physics, Goethe University Frankfurt, 60438 Frankfurt, Germany,
*MarquezReyes@physik.uni-frankfurt.de

² Faculty of Mechanical Engineering and Ship Technology, Gdansk University of Technology,
80-233 Gdansk, Poland

³ Department of Electrical, Electronic and Information Engineering, University of Bologna,
Bologna, Italy

Abstract. In structural health monitoring (SHM) a considerable amount of damage detection algorithms based on guided waves (GW) have been developed. Most of them rely on extensive transducer networks, besides preliminary reference measurements of the structures. This originated a growing demand for hardware simplification and cost reduction of the wave-based SHM methods, driving the conception of new solutions enabling both: the reduction in the amount of sensors required for doing measurements, as well as a diminution of quantity of signals needed for the algorithms to work. The simplification in damage detection procedures can be achieved by using a novel type of special shaped frequency steerable acoustic transducers (FSATs). The spiral shape of these FSATs allows focusing wave energy in a certain direction, which is associated with their excitation frequency. Thanks to this property, presence of damage can be established by identifying signal reflections, while its localization can be determined based on time of flight and the relationship between direction of propagation and its spectral content. This article presents the concept of baseline-free damage detection using FSATs over an aluminium plate with point damage through Finite Element (FE) analysis. Numerical simulations were performed for several cases, varying excitation frequency and damage position.

Keywords: damage detection, frequency steerable acoustic transducer, guided waves, finite element analysis, baseline-free SHM.

1 Introduction

In structural health monitoring (SHM) the main goal is to detect damage or failures over a given structure, determine its location, identify its severity and transfer this information for adequate management. The previous should be done continuously in real time, in an automatized and reliable manner [1]. For this purpose, in structural non-

destructive testing (NDT) a common approach is to install on the surface or embed directly into the structure, arrays of electromechanical devices to perform data collection and generate mechanical elastic guided waves (GW) [2, 3]. This method has also been proven to be successful for homogeneous and even for more complex composite structures [4]. Nowadays Piezoelectric (PZT) based transducers are the most widely used for generation and sensing of ultrasonic guided waves [1], and Lamb waves are particularly attractive in plate-like structures diagnosis [1, 5, 6], given their capability to travel long distances with low attenuation and their sensitivity to various types of defects [7, 8].

The pulse-echo approach is a technique where a single PZT transducer is required for actuation and detection. The waves generated by the transducer propagate across the structure, to be then reflected by discontinuities, such as boundaries or defects of the material. Finally these reflected waves make their way back to the transducer where they are registered by this very device [9]. In SHM is also common to use arrays of three or more transducers in order to uniquely locate damage position over the structure by means of the pitch-catch based imaging, which relies on two separate devices (sensor and actuator). This has proven to be effective in damage detection and location [3, 10]. Nevertheless, the use of multiple transducers, creating networks for this single task, increases the complexity of the whole system, energy consumption, weight and costs.

When propagated waves reach the sensors, the acquired data is interpreted by an imaging algorithm indicating the location of damage. One extensively used of these algorithms is the ellipse method [3, 7]. This approach relies on the calculation of the time of flight (TOF) of the incident and reflected waves to locate defects, and in order for it to accurately locate small defects, a minimum array of three transducers is required for isotropic media; although it is common practice to improve damage mapping by means of larger arrays of sensors [3, 11]. In this paper we present a novel type of baseline-free damage localization approach exploiting angular estimation by a frequency steerable acoustic transducer and time of flight analysis

This article introduces the general methods used for damage detection in SHM, section II presents the pulse-echo approach by means of a new type of frequency steerable acoustic transducers (FSATs). The numerical setup is covered in section III, whereas results for numerical simulations are provided in section IV. Finally the authors' conclusions are presented with the corresponding references for this document.

2 Damage detection with frequency steerable acoustic transducers

The conventional pulse-echo approach, based on the time of flight of the damage reflected wave propagation velocity, the infinite number of possible damage localizations creating a circle in a plane can be indicated for isotropic media. The intersection of circles is an indicator of defect localization. Therefore, the sensitivity of the pulse-echo damage localization algorithms is strongly related to the extent of the transducers network. However, the more sensors in the network, the more data must be processed.

In the case of the FSATs which focus wave energy on a certain direction, uniquely associated with the excitation frequency [12], the procedure of damage detection can be simplified, and the network extent can be reduced. The FSAT frequency directivity behavior is result of the characteristic shape of its electrodes, which is defined in the frequency-wavenumber space [13].

The concept of baseline-free damage detection is presented in Fig. 1. After excitation of the actuator with a signal at defined frequency, a wave propagates in a certain direction (Fig. 1a) and if it encounters damage it reflects. The transducer will register the waves, and the reflection generated by the defect manifests by an additional peak in the signal, preceding the reflections from the boundaries (Fig. 1b). For other frequencies, the reflection from the defect would not be registered or would be characterized by very low amplitude, since it is related to interaction with sidelobes of the FSAT radiation pattern. Next, based on the time of flight, wave velocity and FSAT directivity characteristics (Fig. 1c), the distance between the damage and FSAT as well as the direction can be determined (Fig. 1d).

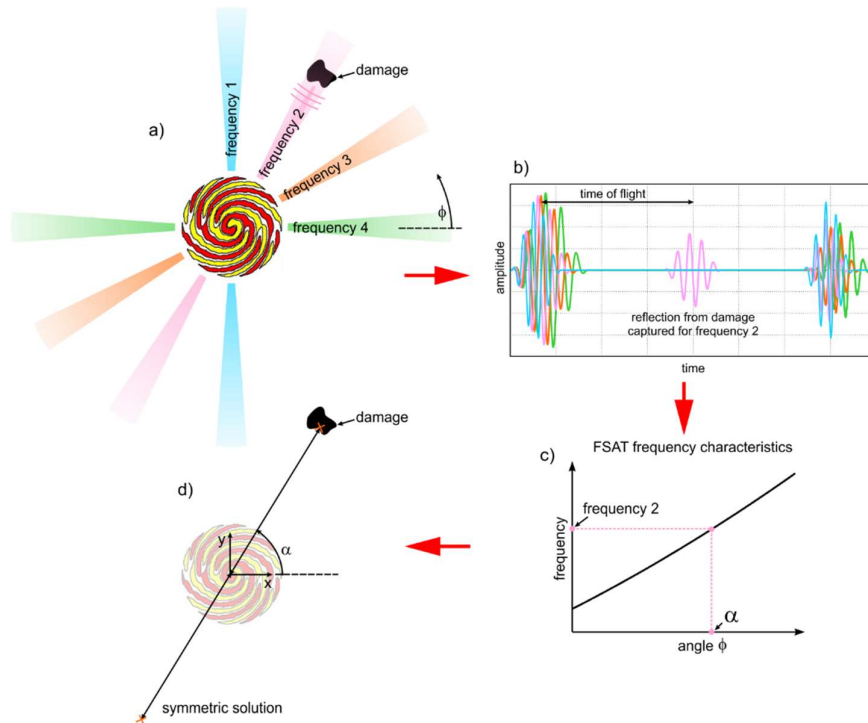


Fig. 1. The concept of damage detection procedure using FSAT: a) excitation using various frequencies, b) analysis of the signals and indicating reflections from damage, c) determination of the direction of propagation based on FSAT frequency characteristics and d) determination of two possible damage localizations.

3 Numerical simulations

3.1 Numerical model

To demonstrate the performances of the novel transducers in damage detection, we have simulated a Lamb wave propagation in a 3D numerical model of a 1-mm thick aluminum plate characterized by the following material parameters: elastic modulus 70 GPa, Poisson's ratio 0.3 and material density 2700 kg/m^3 . The dimensions of the considered plate were 350 mm x 500 mm. To which a piece of PIC255 piezoelectric material, with customized shaped electrodes, was installed, as shown in Fig. 3. This tailored shaped transducer presents directional capabilities, described in the following section. The excitation was applied perpendicular to the plate surface, which triggered antisymmetric A_0 mode propagation. The dispersion curve for A_0 mode is presented in Fig. 2.

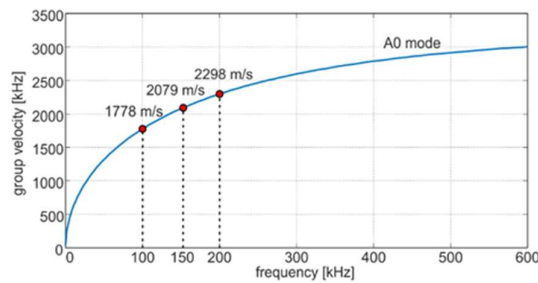


Fig. 2. Dispersion curve for A_0 mode propagating in aluminium plate ($E = 70 \text{ GPa}$, $\nu = 0.3$, $\rho = 2700 \text{ kg/m}^3$)

The numerical simulations were performed with commercial FEM-based software COMSOL. For accurate modeling of mechanical guided waves propagation and the piezoelectric effect of the PZT transducer, two physics modules were incorporated in this study: "Structural Mechanics" and "Electrostatics". The excitation was applied as time-dependent voltage in the form of an amplitude modulated 5-cycle sine function. To minimize the influence of side reflections from plate edges, the build-in low reflection boundary condition was used at the plate boundaries.

3.2 FSAT directivity characteristics

The analysis studying the possibility of performing damage detection was preceded by numerical simulations for undamaged aluminum plate, this aiming to determine the directivity characteristics and radiation patterns that were to be used in the following steps of the investigation. To exemplify the preferential propagation directions of the FSAT accordingly to the excitation frequency, radiation patterns for three different frequencies (100, 150, and 200 kHz) are depicted in Fig. 3.

To obtain these patterns, we extracted the maximum amplitude value of the out-of-plane displacements caused by wave motion registered over a circle with a radius of 50 mm around the FSAT. Now, based on the obtained patterns, the directivity characteristics in the form of an angle-frequency relationship has been defined (Fig. 3d).

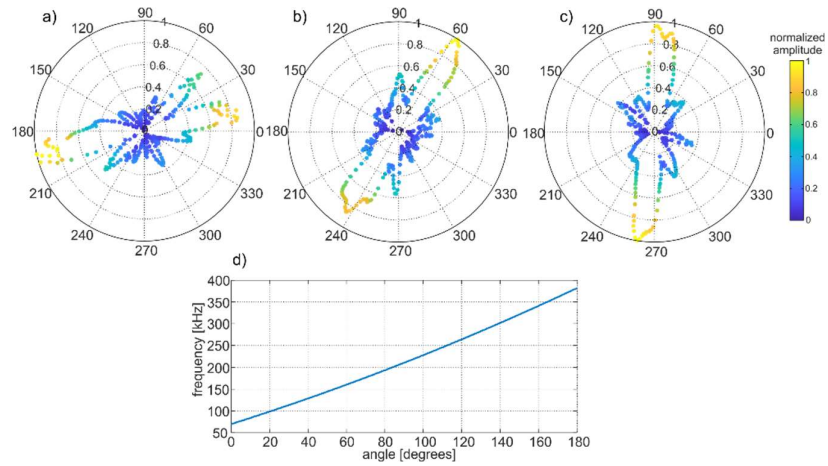


Fig. 3. Directivity pattern at a) 100 kHz, b) 150 kHz c) 200 kHz and d) the angle-frequency relationship for FSAT.

3.3 Damage scenarios

Based on the obtained results for the FSAT, the parameters for damaged aluminum plates investigated during the numerical campaign were established. The analysis concerned three different damage scenarios, varying in defect localization. The angle between the horizontal axis and the line connecting the middle of the plate with the center of the damage was equal to 90, 60, and 30 degrees, respectively. The damage was modeled as cut-through plate thickness in every case; the distance between FSAT and damage (150 mm), as well as the damage size (15 mm x 15 mm) were defined. The simulations were performed for three excitation frequencies corresponding to chosen angles: 100 kHz, 150 kHz and 200 kHz (compare Fig. 4). In total, nine cases were tested.

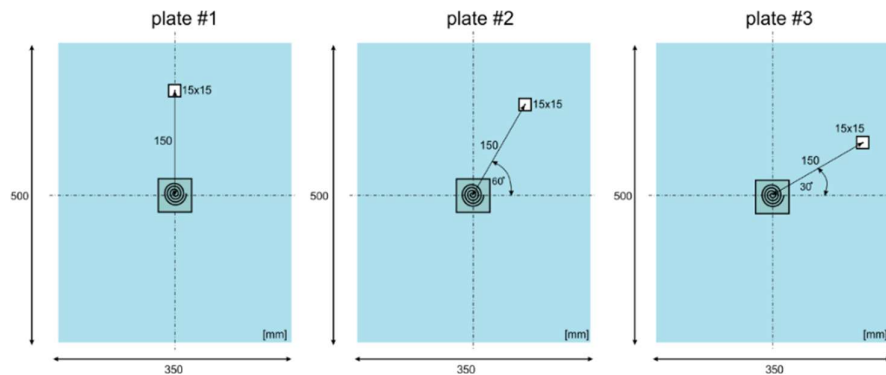


Fig. 4. Geometry of the numerical models: damage scenarios with variable damage locations.

4 Results of damage detection and localization

The results of the simulations for plates #1 -#3 are presented in the form of snapshots at selected time instants (Figs. 4 - 6). The preferential radiation patterns are visible in each case. Moreover, we can also observe wave reflection from the damage in each case, regardless of the excitation frequency. The main difference is the amplitude of the reflection. If the damage is located in the direction of the main lobe, the amplitude is relatively high and comparable to the amplitude of the main lobe. In other cases, we observe the reflection of the low-amplitude side-lobe. This effect can be clearly observed in the first damage scenario, where damage is localized in the direction of the main lobe of 200 kHz (Fig. 5c). However, in some cases (see Fig. 6a $t = 0.1$ ms) the interaction with the sidelobe results also in high-amplitude reflection, which can influence the damage localization in the further stages of the analysis.

The differences in amplitudes are also observed in signals registered by the FSAT, depicted in Fig. 8. The amplitude was normalized concerning the input wave packet.

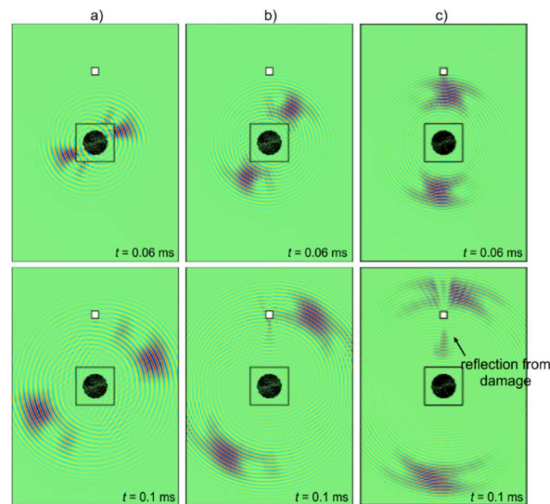


Fig. 5. Visualization of wave propagation in plate#1 after excitation with the frequency of a) 100 kHz, b) 150 kHz and c) 200 kHz.

The results of the signal processing are summarized in Table 1. As expected, the strongest reflections were captured for various frequencies depending on the location of the damage. The times of flight for the reflections were calculated as the peak-to-peak value and next, based on the TOFs and the wave velocities, determined by solving the Lamb equation, the distance between the FSAT and the defect was calculated. It can be seen that in every case, the distance was estimated correctly, varying from 12.6 cm to 15.6 cm. The last column contains the normalized amplitudes of the reflections. The rows with the highest amplitude values have been highlighted and the damage was localized based on the data contained therein (Fig. 9).

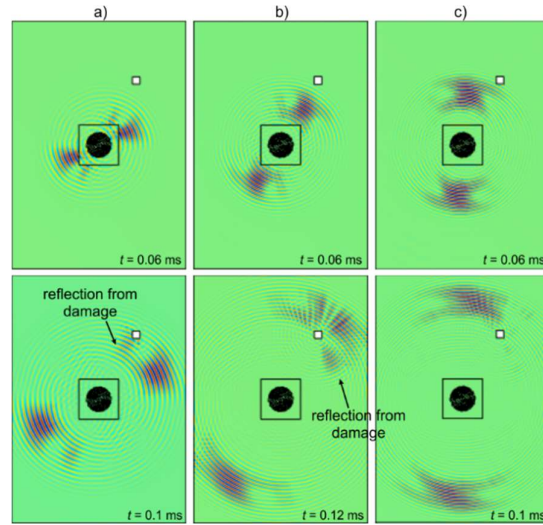


Fig. 6. Visualization of wave propagation in plate#2 after excitation with the frequency of a) 100 kHz, b) 150 kHz and c) 200 kHz.

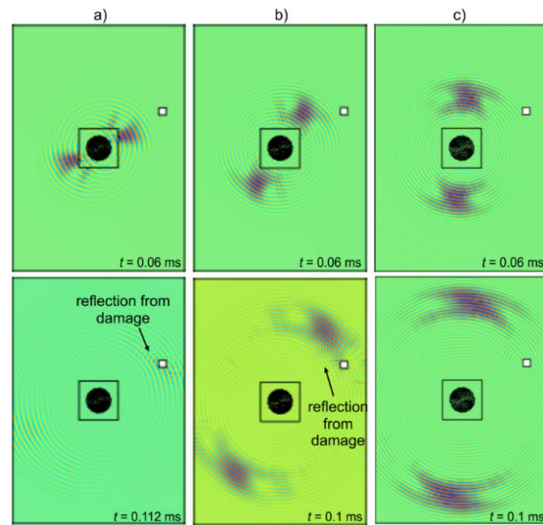


Fig. 7. Visualization of wave propagation in plate#3 after excitation with the frequency of a) 100 kHz, b) 150 kHz and c) 200 kHz.

For clarity, Fig. 9 contains only one possible damage location, but it should be noted that the wave patterns generated by FSAT are antisymmetric, so based on only one signal we obtain two antisymmetric solutions. In the considered case the damages were located in the first quarter, so the alternative solution would be located also in the third

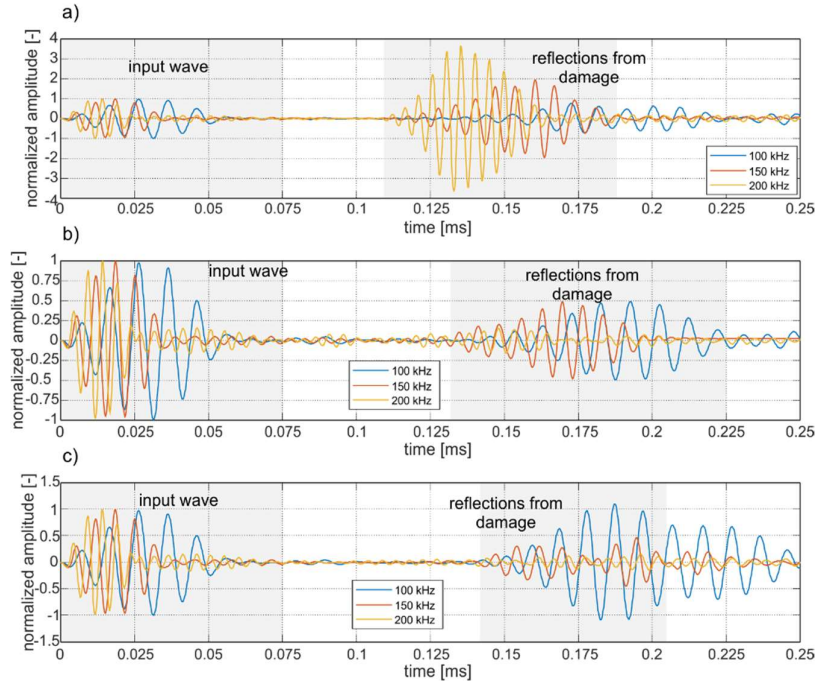


Fig. 8. Wave propagation signals registered by FSAT at a) plate#1, b) plate#2 and c) plate#3.

Table 1. Results of signal processing – damage detection and localization.

Model	Frequency [kHz]	TOF of reflection from damage [ms]	Distance from FSAT [m]	Amplitude value [-]
Plate#1	100	0.1440	0.126	0.790
	150	0.1432	0.147	2.000
	200	0.1207	0.138	3.670
Plate #2	100	0.1646	0.144	0.500
	150	0.1516	0.156	0.490
	200	0.1363	0.156	0.159
Plate #3	100	0.1560	0.136	1.114
	150	0.1387	0.142	0.326
	200	0.1315	0.150	0.080

quarter. The angles between the horizontal axis and the direction of the main lobe were determined based on the curve in Fig. 3d. The determined damage locations can be found satisfactory, especially if we consider the limited amount of necessary data. However, in any case, the estimated defect localization does not coincide perfectly with the actual ones. The main reason for the discrepancies is the limited range of the employed frequencies. After rough localization of the defect, the frequency range could

be modified to increase the accuracy i.e., in the case of plate#1 and finding that excitation of 200 kHz results in the strong reflection, in the next step the procedure could be repeated for frequencies from 180 to 220 kHz.

This approach would be also useful in the case of ambiguous results as in the case of plate#2. For this plate, the reflection amplitude was comparable for two frequencies (100 and 150 kHz) and thus Fig 8b contains only the range where the damage can be located instead of the concrete point. The analysis of the numerical visualizations demonstrated that high-amplitude reflection for 100 kHz resulted from interaction of a high-energy sidelobe, which is also clearly visible in the directivity pattern in Fig. 3a.

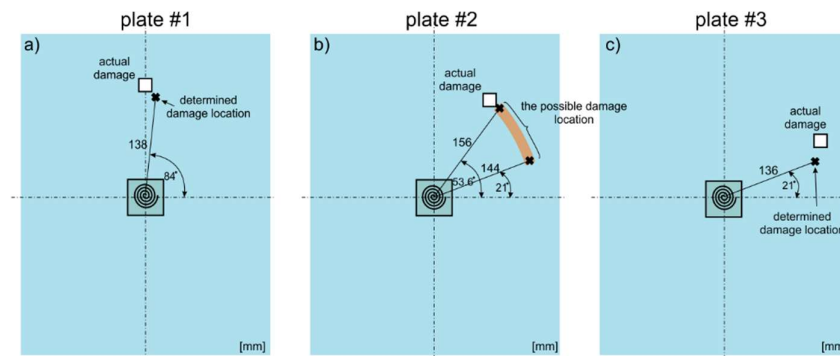


Fig. 9. Results of damage detection and localization compared with actual models' geometry: a) plate #1, b) plate #2, and c) plate #3.

5 Conclusions and future plans

This article presents the results provided by FEM analysis concerning wave propagation in plate-like structures with damage. It is clear that typical sensor networks can be significantly reduced by using the inherent steerable properties of novel FSATs. The possible damage localization was determined by using the standard pulse-echo approach, combined with the assessment of reflection strength. For future developments, we aim to analyze the possibility of using pulse excitation resulting in the propagation of multiple frequencies simultaneously. Moreover, it is also crucial to consider the problem of variable sensitivity of damage detection. FSATs propagate various frequencies in different directions which also results in the propagation of waves varying in wavelength, which implies that the effectiveness of damage detection depends not only on its size but also on its location with respect to the FSAT.

References

1. Mitra, M., Gopalakrishnan S.: Guided wave based structural health monitoring: A review. *Smart Materials and Structures* 25(5), 053001–053027 (2016).

2. Moll, J., Golub, M.V., Glushkov, E., Glushkova, N., Fritzen, C.: Non-axisymmetric Lamb wave excitation by piezoelectric wafer active sensors. *Sensors and Actuators A174*, 173–180 (2012).
3. Zima, B., Rucka, M.: Guided waves for monitoring of plate structures with linear cracks of variable length. *Archives of Civil and Mechanical Engineering* 16(3), 387–396 (2016).
4. Moll, J., Kexel C., Kathol, J., Fritzen C., Moix-Bonet M., Willberg, C., Rennoch, M., Koerdt, M.: Guided Waves for Damage Detection in Complex Composite Structures: The Influence of Omega Stringer and Different Reference Damage Size. *Applied Sciences* 10(9), 3068–3088 (2020).
5. Rose, J.L.: Ultrasonic Guided Waves in Structural Health Monitoring. *Key Engineering Materials* 270, 14-21 (2004).
6. Sun, Y., Xu, Y., Li, W., Li, Q., Ding, X., Huang, W.: A Lamb Waves Based Ultrasonic System for the Simultaneous Data Communication, Defect Inspection, and Power Transmission. *IEEE Transactions on Ultrasonics, Ferroelectrics, and Frequency Control*. 68(10), 3192–3203 (2021).
7. Zima, B.: Damage detection in plates based on Lamb wavefront shape reconstruction. *Measurement* 177, 109206–109228 (2021).
8. Kexel, C., Testoni, N., Zonzini, F., Moll, J., De Marchi, L.: Low-Power MIMO Guided-Wave Communication. *IEEE Access* 8, 217425–217436, (2020).
9. Wandowski, T., Malinowski, P., Ostachowicz W. M.: Damage detection with concentrated configurations of piezoelectric transducers. *Smart Materials and Structures* 20(2), 025002–025015, (2011).
10. Sohn, H., Park, H. W., Law, K. H., Farrar, C. R.: Combination of a time reversal process and a consecutive outlier analysis for baseline-free damage diagnosis. *Journal of Intelligent Material Systems and Structures* 18(4), 335–346 (2007).
11. Deraemaeker, A., Preumont, A.: Vibration based damage detection using large array sensors and spatial filters. *Mechanical Systems and Signal Processing* 20, 1615–1630 (2006).
12. Senesi, M., Baravelli, E., De Marchi, L., Ruzzene, M. : Experimental demonstration of directional GW generation through wavenumber-spiral Frequency Steerable Acoustic Actuators. In 2012 IEEE International Ultrasonics Symposium, pp. 2694-2697, Dresden, Germany (2012).
13. Baravelli, E., Senesi, M., Ruzzene, M., De Marchi, L.: Fabrication and Characterization of a Wavenumber-Spiral Frequency-Steerable Acoustic Transducer for Source Localization in Plate Structures. *IEEE TRANSACTIONS ON INSTRUMENTATION AND MEASUREMENT* 62(8), 2197–2204 (2013).

Acknowledgments

OMR and JM gratefully acknowledge financial support by the German Research Foundation (DFG) under grant 349435502. MM and LDM gratefully acknowledge funding from the European Union’s Horizon 2020 project Guided Waves for Structural Health Monitoring (GW4SHM, GA: 860104). BZ gratefully acknowledges the support of the Foundation for Polish Science (FNP).